

UCRL-9867  
Limited distribution

UNIVERSITY OF CALIFORNIA  
Lawrence Radiation Laboratory  
Berkeley, California  
Contract No. W-7405-eng-48

**INTERACTIONS OF LAMBDA WITH PROTONS**

Gideon Alexander, Jared A. Anderson, Frank S. Crawford, Jr.,  
William Laskar, and Lester J. Lloyd

September 21, 1961

## INTERACTIONS OF LAMBDA'S WITH PROTONS\*

Gideon Alexander,<sup>†</sup> Jared A. Anderson, Frank S. Crawford, Jr.,  
William Laskar, and Lester J. Lloyd

Lawrence Radiation Laboratory  
University of California  
Berkeley, California

September 21, 1961

In the course of an experiment to study the associated production processes



and



we have examined subsequent  $\Lambda$  interactions in hydrogen of the types



In this Letter we present results for reactions (3) and (4), based on a sample of 5000  $\Lambda$ 's produced in the Alvarez 72-in. hydrogen bubble chamber. [We postpone discussion of reaction (5) to a later publication.]

In addition, we set an upper limit to the pion-producing reactions



and



The  $\Lambda$  "beam" momentum extends from 400 to 1000 Mev/c, and corresponds to the associated production processes (1) and (2) for incident  $\pi^-$ 's of 1035 Mev/c. The distribution of  $\Lambda$  momentum versus pathlength is shown in Fig. 1. It includes two cutoff corrections: (a) single  $V^0$  decays of  $K^0$  or  $\Lambda$  (without subsequent scatter) are rejected if the neutral particle travels less than 0.5 cm before decaying; (b) only those  $\Lambda$  interactions that occur within 10 cm of the production point are accepted. Cutoff (a) serves to exclude spurious  $V^0$ 's due to two-prong events. Cutoff (b), while including most of the  $\Lambda$  path length before decay, serves to minimize the geometrical escape correction, and helps to exclude random background recoil protons from candidacy.

Lambda interactions that are followed by the charged decay  $\Lambda \rightarrow p + \pi^-$  are detectable whether or not the associated  $K^0$  undergoes charged decay. Interactions followed by the neutral decay  $\Lambda \rightarrow n + \pi^0$  are also detectable and are used, provided that the  $K^0$  decays via the charged mode. The kinematics and measuring errors are such that there is no difficulty in distinguishing between reactions (3) and (4).

Some of the interactions were found by scanners in the first scan. However, the main search for interactions consisted of (a) a systematic examination on the scanning table of all single and double  $V^0$  events which failed to satisfy the kinematics for production via reactions (1) and (2); and (b) an examination on the scanning table of all single  $V^0$  events where the decaying neutral is identified as a  $K^0$ . Here one looks for a recoil proton starting from the line of flight of the  $\Lambda$ .

Recoil protons of less than 0.5 cm are difficult to detect, and have been excluded. Our elastic-scattering cross section [Reaction (3)] therefore does not include small angle scatters of the  $\Lambda$ . The excluded angular region depends on the momentum of the incident  $\Lambda$ , and is indicated by the shaded region in Fig. 2.

The correction to the integrated cross section depends on the shape of the angular distribution. The elastic-scattering cross sections include a cutoff correction for which uniformity in  $\cos \theta_{\Lambda}$  (c.m.) and  $P_{\Lambda}$  (lab) is assumed. From Fig. 2 we see that, within the limited statistics, these assumptions are satisfied. The correction factor amounts to 1.074 for  $P_{\Lambda}$  (lab) from 400 to 638 Mev/c, and 1.028 for  $P_{\Lambda}$  (lab) above 638 Mev/c, the threshold for  $\Sigma^0$ -p production.

In the cases of the endothermic processes (4), (5), and (6), the proton range exceeds 0.5 cm for all production angles over the entire range of  $P_{\Lambda}$  (lab), so that there is no corresponding cutoff correction.

Details of the individual events are found in Table I. Figure 2 shows the laboratory momentum of the incident  $\Lambda$  and the c.m. angle of the final hyperon (relative to the incident  $\Lambda$ ) for each event. Table II gives our cross-section results. The elastic-scattering cross section is given for the entire momentum interval, and separately for the intervals below and above 638 Mev/c, the threshold for reaction (4). The upper limit given for the pion-producing reaction (6) is the cross section that would correspond to finding a single event instead of the number (zero) actually found.

Our elastic-scattering cross section can be compared with the previous result of Crawford et al.,<sup>1</sup> obtained in substantially the same momentum interval. Based on four events, they found a cross section of  $40 \pm 20$  mb, which is not in disagreement with our result of  $22.3 \pm 5.9$  mb.

Information from study of hyperfragments has been used by Kovacs and Lichtenberg<sup>2</sup> to calculate the elastic-scattering cross section at 416 Mev/c (75 Mev) and at 598 Mev/c (150 Mev). They chose a phenomenological central potential with a hard core and considered only angular momenta of  $\leq 2$ . Their calculated results are 26 and 21 mb at 416 and 598 Mev/c, respectively, when no spin-orbit term is included, and 34 and 32 mb when spin-orbit interaction is included. Our measured value of  $24.7 \pm 9.3$  mb for

the interval 400 to 638 Mev/c is compatible with either calculated result. Thus we agree with the prediction from hyperfragment data, but cannot distinguish between the presence or absence of spin-orbit terms.

In the Doublet Approximation (DA),<sup>3</sup> the  $\Sigma$  -  $\Lambda$  mass difference is neglected and  $\Sigma^0$  and  $\Lambda$  are combined into the two doublets  $[N_2 = [\Sigma^+, (\Lambda - \Sigma^0)/\sqrt{2}]$  and  $N_3 = [(\Lambda + \Sigma^0)/\sqrt{2}, \Sigma^-]$ . Both  $N_2$  and  $N_3$  have the same coupling to the pion field. This pion coupling need not be the same as that of the nucleon doublet  $N_1 = [p, n]$ . In addition, a new quantum number is introduced which prevents mixing of the doublets.<sup>3</sup> (For instance,  $\Sigma^- + p \rightarrow \Sigma^+ + n + \pi^-$  is forbidden in DA). The mass difference between  $N_2$  or  $N_3$  and the nucleon  $N_1$  is not neglected.

One can then show that

$$2[\sigma(\Lambda p \rightarrow \Lambda p) + \sigma(\Lambda p \rightarrow \Sigma^0 p)] = \sigma(\Sigma^+ p \rightarrow \Sigma^+ p) + \sigma(\Sigma^- p \rightarrow \Sigma^- p). \quad (7)$$

Of course, Eq. (7) can only be valid at energies high enough that the actual  $\Sigma$  -  $\Lambda$  mass difference is negligible compared with the c.m. kinetic energy. For instance, Eq. (7) is certainly inapplicable below threshold for  $\Lambda p \rightarrow \Sigma^0 p$ . As a first approximation to a test of Eq. (7), we compare our results for the reactions on the left side of Eq. (7) to those of Stannard<sup>4</sup> for those on the right side. We consider the  $\Lambda p \rightarrow \Lambda p$  cross section only for  $P_\Lambda$  (lab) above 638 Mev/c, the threshold for reaction (4). Our range of total c.m. energy corresponds to a  $\Sigma$ -p c.m. momentum range of 0 (at threshold) to 314 Mev/c [for  $P_\Lambda$  (lab) of 1000]. Stannard's results correspond to a  $\Sigma$ -p c.m. momentum range of 0 to about 600 Mev/c.

We find

$$2[\sigma(\Lambda p \rightarrow \Lambda p) + \sigma(\Lambda p \rightarrow \Sigma^0 p)] = 57 \pm 18 \text{ mb.}$$

Stannard finds

$$\sigma(\Sigma^+ p \rightarrow \Sigma^+ p) + \sigma(\Sigma^- p \rightarrow \Sigma^- p) = 48 \pm 17 \text{ mb.}$$

Within the statistical errors, the prediction [Eq. (7)] of the Doublet Approximation is well satisfied.

In the theory of Global Symmetry (GS),<sup>5</sup> the assumption (in addition to those of DA) is made that the pion coupling of  $N_2$  and  $N_3$  is the same as that of the nucleon  $N_1$ , and the mass difference between  $N_2$  or  $N_3$  and  $N_1$  is neglected. One can then predict  $N_1 - N_2$  or  $N_1 - N_3$  interactions from  $N_1 - N_1$  (nucleon-nucleon) interactions. De Swart and Dullemond have used potentials that fit available nucleon-nucleon scattering data, in linear combinations prescribed by GS, to predict cross sections for hyperon-nucleon interactions.<sup>6</sup> They take exactly into account the  $\Sigma - \Lambda$  mass difference in the kinematics (but neglect the  $\Sigma$ -nucleon mass difference). Their predictions for  $\Lambda$ -p elastic scattering and for  $\Sigma^0$ -p production [reaction (4)] are shown in Fig. 3, together with our experimental results. Within statistics, our cross sections agree with the predictions of GS.

De Swart and Dullemond also predict angular distributions for  $\Lambda$ -p elastic scattering at 475, 640, and 815 Mev/c. These momenta cover our range of  $P_\Lambda$  fairly well (see Fig. 1). With our limited statistics we can check at most a single parameter of the angular distribution. We examine our ratios for forward to backwards scattering (F/B) and for polar to equatorial scattering (P/E). Since we see no strong momentum dependence in the elastic-scattering cross section, and since the predicted angular distributions do not vary drastically over our momentum range, we average with equal weight the theoretical predictions for F/B and P/E and compare them with our entire sample of 14 events.

For F/B we find  $7/7 = 1.0 \pm 0.5$ . The prediction of GS is 1.5.

For P/E we find  $9/5 = 1.8 \pm 1.0$ . The GS prediction is 2.0.

It is a pleasure to acknowledge the guidance and encouragement of Prof. Luis W. Alvarez.

REFERENCES AND FOOTNOTES

\* This work was done under the auspices of the U. S. Atomic Energy Commission.

† International Cooperation Administration Fellow on leave of absence from the Israel Atomic Energy Commission Laboratories, Rehovoth, Israel.

1. F. S. Crawford, M. Cresti, M. L. Good, F. T. Solmitz, M. L. Stevenson, and H. K. Ticho, *Phys. Rev. Letters* 2, 174 (1959).
2. J. S. Kovacs and D. B. Lichtenberg, *Nuovo cimento* 13, 371 (1959).
3. A. Pais, *Phys. Rev.* 110, 574 (1958), and Lawrence Radiation Laboratory Report UCRL-9460, October 27, 1960 (unpublished); *Nuovo cimento* 18, 1003 (1960).
4. F. R. Stannard, *Phys. Rev.* 121, 1513 (1961).
5. E. P. Wigner, *Proc. Natl. Acad. Sci. U.S.* 38, 449 (1952); J. Schwinger, *Ann. Phys.* 2, 407 (1957); M. Gell-Mann, *Phys. Rev.* 106, 1296 (1957).
6. J. J. de Swart and C. Dullemond, University of Rochester Report NYO-9746, June 20, 1961 [*Ann. Phys.* (to be published)].

Table I. Details of the interactions.

Frame	Initial lab momentum of $\Lambda$ (Mev/c)	C. m. momentum		Cos $\theta_Y$ (c. m.)
		Initial	Final	
<b>A. <math>\Lambda + p \rightarrow \Lambda + p</math></b>				
602103	418	188	188	+ 0.35
722504	421	189	189	- 0.92
739246	436	196	196	+ 0.37
865515	447	200	200	+ 0.19
818550	483	216	216	- 0.94
586135	532	236	236	+ 0.65
537508	555	246	246	- 0.64
834420	678	297	297	+ 0.23
864246	684	300	300	+ 0.58
814534	787	341	341	- 0.99
602317	796	345	345	- 0.99
857282	822	355	355	+ 0.73
539021	921	393	393	- 0.99
724478	977	413	413	- 0.20
<b>B. <math>\Lambda + p \rightarrow \Sigma^0 + p</math></b>				
861205	646	284	42	- 0.11
586381	788	341	193	- 0.30
692127	943	401	285	+ 0.78



Table II. Summary of cross-section results.

Reaction	$P_{\Lambda}$ (lab) (MeV/c)	No. of events	$\Lambda$ path length (cm)	Cross section (mb)
$\Lambda + p \rightarrow \Lambda + p$	400 - 1000	14	18770	$22.3 \pm 5.9$
$\Lambda + p \rightarrow \Lambda + p$	400 - 638	7	8700	$24.7 \pm 9.3$
$\Lambda + p \rightarrow \Lambda + p$	638 - 1000	7	10070	$20.4 \pm 7.7$
$\Lambda + p \rightarrow \Sigma^0 + p$	638 - 1000	3	10070	$8.5 \pm 4.9$
$\Lambda + p \rightarrow \left\{ \begin{array}{l} \Lambda + p + \pi^0 \\ \Lambda + n + \pi^+ \end{array} \right\}$	880 - 1000	0	1986	$< 14 \pm 14$

### FIGURE LEGENDS

**Fig. 1.** Distribution of  $\Lambda$  path length versus momentum. The arrows indicate the thresholds for reactions (4) and (6).

**Fig. 2.** Details of the interactions. Solid circles indicate elastic scatters [reaction (3)]. Open circles represent  $\Sigma^0 - p$  production [reaction (4)]. The shaded region corresponds to elastic scattering in which the recoil proton has a range of  $< 5$  mm.

**Fig. 3.** Comparison of our experimental results with the predictions (based on Global Symmetry) of de Swart and Dullemond.<sup>6</sup> The upper curve and the solid circles represent elastic scattering. The lower curve and open circle correspond to  $\Sigma^0 - p$  production.

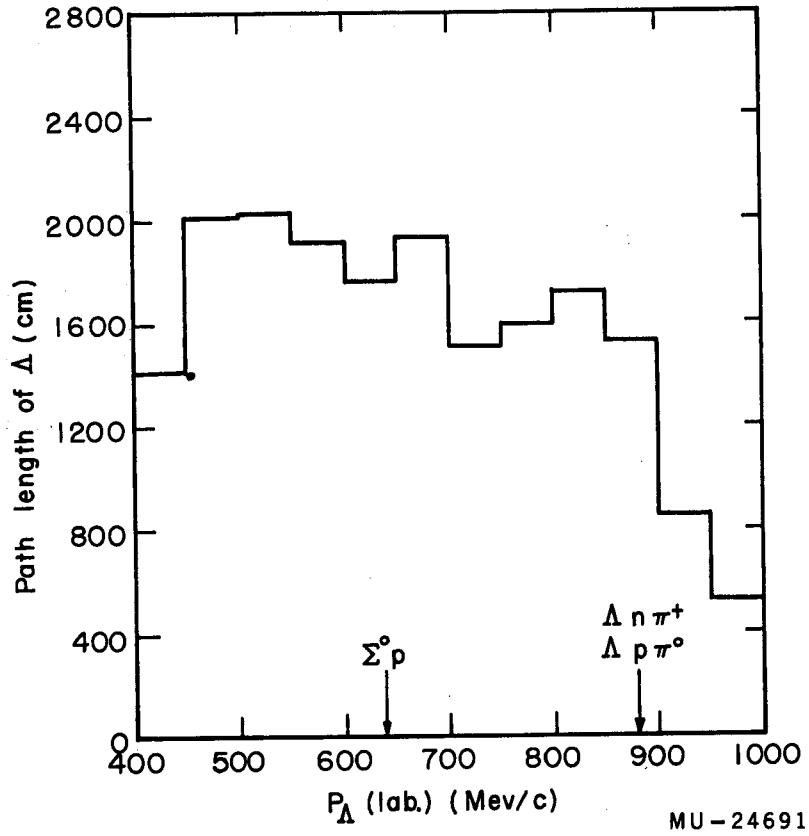


Fig. 1

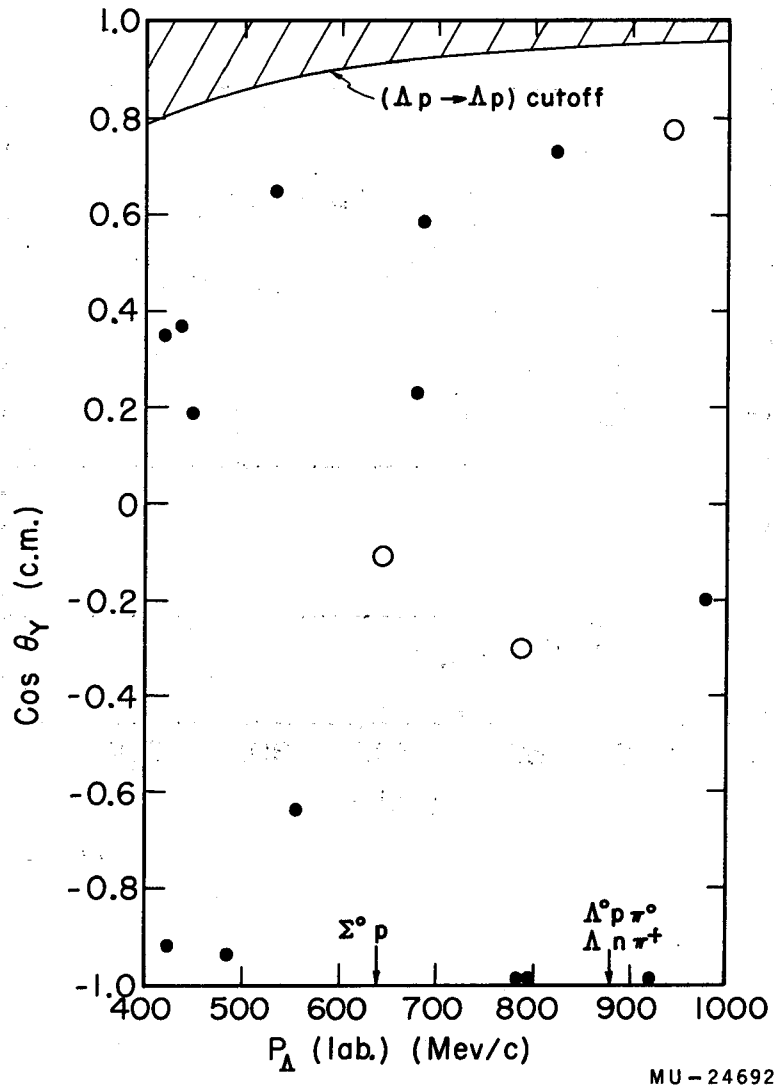
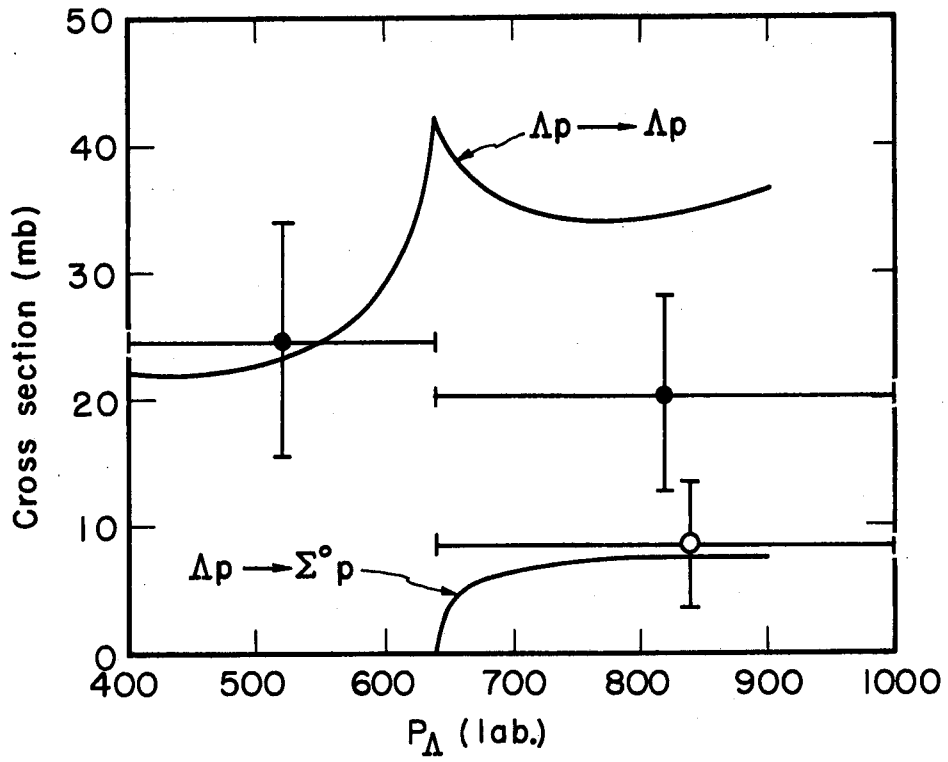


Fig. 2



MU-24693

Fig. 3

This report was prepared as an account of Government sponsored work. Neither the United States, nor the Commission, nor any person acting on behalf of the Commission:

- A. Makes any warranty or representation, expressed or implied, with respect to the accuracy, completeness, or usefulness of the information contained in this report, or that the use of any information, apparatus, method, or process disclosed in this report may not infringe privately owned rights; or
- B. Assumes any liabilities with respect to the use of, or for damages resulting from the use of any information, apparatus, method, or process disclosed in this report.

As used in the above, "person acting on behalf of the Commission" includes any employee or contractor of the Commission, or employee of such contractor, to the extent that such employee or contractor of the Commission, or employee of such contractor prepares, disseminates, or provides access to, any information pursuant to his employment or contract with the Commission, or his employment with such contractor.